Lap joining 5052 aluminum alloy to Ti6Al4V titanium alloy by GTAW process with AlSi12 filler wire

Akhtar Awais, Dong Honggang, Xia Yueqing, Li Peng

Akhtar Awais, 董红刚, 夏月庆, 李鹏

School of Materials Science and Engineering, Dalian University of Technology, Dalian 116024, China

Received 23 June 2020; accepted 17 August 2020

Abstract The process of gas tungsten arc welding (GTAW) is applied with AlSi12 filler metal to weld 5052 aluminum alloy and Ti6Al4V titanium alloy in lap configuration. The welded lap joints showed dual features of welding and brazing on the aluminum and titanium parts of the joint, respectively. The continuous reaction layer established in the brazed area and its chemical composition by EDS analysis revealed that the intermetallic compounds (IMCs) layer of $Ti(Al, Si)_3$ phase formed and aluminum was partially substituted by silicon. The thickness of reaction layer differed from 1μm to 3.5 μm with increase in welding heat input accordingly. Al, Ti and Si elements in the weld region and IMCs layer were recognized by analysis of EPMA. The maximum tensile shear strength attained at the optimized welding heat input was 376 N/mm and the joint fractured from 5052 aluminum alloy base metal. Furthermore, the microhardness was measured, and the hardness was higher at the Al/Ti interface than in the weld seam and Ti6Al4V alloy base metal because of the development of IMCs.

Key words gas tungsten arc welding, aluminum alloy, titanium alloy, intermetallic compound, mechanical property

0 Introduction

Titanium alloys have wide applications in aerospace and aircraft industrial sectors due to remarkable combination of its properties such as outstanding mechanical strength, excellent corrosion resistance and high specific strength[1]. Aluminum alloys having lightweight with two-thirds of titanium alloys density and other favorable properties have extensive potential in automobile and transportation industries for weight reduction purposes[2]. Both Ti and Al alloys are used in industrial field to improve strength and reduce weight[3]. Ti/Al hybrid structures have dominance of lightweight requirements along with strength as compared with individual material. However, it is extremely challenging in joining the aluminum and titanium thermally owing to huge differences in melting points, crystallographic structures, linear expansion coefficients and heat conductivities. The inevitable brittle IMCs formation during the welding process has a substantial influence on the joint efficiency. The increased concentration of intermetallic compounds at the Ti/Al joint interface, deteriorates the welded joint[4]. Therefore, appropriate thickness of Ti-Al intermetallic phase is indispensable for the strong joint.

Several welding procedures have been used to produce Ti/Al butt joints such as laser welding-brazing technology[5], tungsten inert gas welding[6] and brazing[7].Some solid state welding techniques have been practiced including explosive welding[8], diffusion bonding[9] and friction stir welding[10] for dissimilar joining Ti/Al alloys in lap configuration. However, these processes have narrowed practical implementation owing to productivity and high cost, extensive plastic distortion related to friction welding and limitations in the configuration of the components[11].

Gas tungsten arc welding (GTAW), being an efficacious and resilient welding technique, is featured of its in-

Foundation item: Project was supported by the National Natural Science Foundation of China (51674060) and the Collaborative Innovation Center of Major Machine Manufacturing in Liaoning.

Corresponding author: Dong Honggang, (1975 −), Ph.D. Professor. Mainly engaged in dissimilar materials welding. E-mail : donghg@dlut.edu.cn

doi: 10.12073/j.cw.20200623001

creased efficiency, productivity and superior joint quality. This technology delivers significant potential to join materials subjected to its slight dependence on expensive apparatus and complex welding methods[12]. Moreover, dissimilar metals having large differences in thermal-physical properties can be successfully joined by this process e.g. magnesium and titanium[13].

Lap joint have been produced between Ti/Al alloys with aid of zinc foil by TIG welding-brazing process[11]. The Ti/Al joints showed both characteristics of welding and brazing. The resultant lap joint exhibited the occurrence of fusion welding between base metal of Al alloy and filler metal whereas brazing phenomena occurred at the interface of Ti alloy and filler metal. The joint fractured in the weld zone which specified that the brazed interface of Ti/Al remained stronger during the tensile testing.

Nevertheless, the study associated with GTAW of Al5052/Ti6Al4V in lap joint formation without assistance of interlayer is insufficient. In this study, robust joining of Ti6Al4V titanium alloy and 5052 aluminum alloy were successfully accomplished utilizing AlSi12 filler wire by GTAW process without the use of interlayer. The effect of welding heat input on the microstructures, tensile and fracture properties, accordingly, were investigated by experimental examinations.

1 Experimental procedure

An automatic GTAW machine (YC500WX4N) was employed in the current study to carry out welding experiment. Two dissimilar base metals Ti6Al4V titanium alloy (Ti6Al4V) and 5052-H32 aluminum alloy (Al5052) sheets were chosen for welding and fashioned with same dimensions of 200 mm × 80 mm × 2 mm. AlSi12 wire was applied as the filler metal with 1.2 mm diameter. The nominal composition of base materials and filler metal are listed in Table 1. Prior to GTAW, overlying sides of base metals were ground

Table 1 Nominal compositions of Al5052, Ti6Al4V and filler wire (wt.%)

Material	Al	Ti	Si	Mg	V	Mn	Fe	Zn
Al5052	Balance	0.14	0.45	2.15	–	0.06	0.32	–
Ti6Al4V	6.26	Balance	–	–	4.40	–	0.21	–
Filler wire	Balance	0.15	12.0	0.1	–	0.15	<0.80	0.20

to remove oxide layers and afterward cleaned with acetone and dried. Both workpieces of Al5052/Ti6Al4V in the overlap arrangement were assembled with Al alloy workpiece positioned on the upper side of Ti alloy as indicated in Fig.1a. Argon shielding gas was applied from the torch on the surfaces of workpiece to prevent the oxidization of liquid metals during welding. The optimized experimental welding parameters that have been practiced in the current work are given in Table 2.

Table 2 Experimental welding parameters during the Al5052 / Ti6Al4V joining by GTAW process

Welding current I/A	Welding speed v/(mm·s^{-1})	Wire feed speed v_s/(mm·s^{-1})	Flow rate of shielding gas Q/(L·min^{-1})
60-90	1	18	12

Subsequent to welding process, resultant Al5052/Ti6Al4V joints were fabricated into the rectangular form with a width of 20 mm as exhibited in Fig.1b. The tensile shear strength of the weldments was evaluated at a continual 1mm/min rate with (DNS-100) universal tensile testing equipment. In order to promote the accuracy and consistency of the testing joints, three tensile specimens were prepared for every set of welding parameter. Metallographic samples were also cut from the cross section of the weldment for microscopic examination. After standardized grinding and polishing methods, the microstructural samples were inspected by OM and SEM. Investigation of the Al5052/Ti6Al4V interfacial area was executed by electron probe microanalysis (EPMA) without etching to ascer-

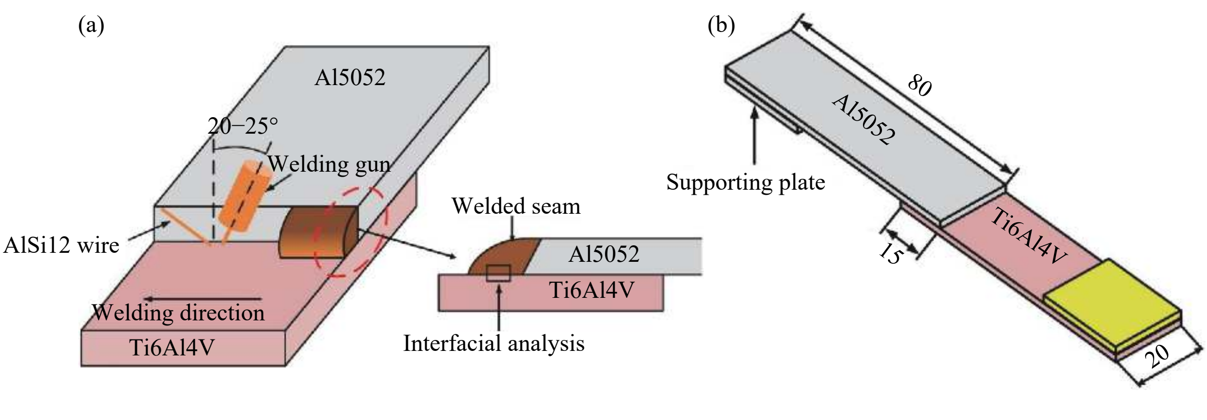

Fig. 1 Illustration of GTAW process and tensile sample (a) Schematic of GTAW (b) Tensile-shear test sample dimensions (mm)

tain the alloying elements distribution in and surround the interface and to further recognize the IMCs formation across the joint due to diffusion of elements. Fractured sides of the overlap joints were analyzed by SEM equipped with EDS. The microhardness evaluation of the Al5052/Ti6Al4V joint at different regions was conducted by microhardness testing machine, along and across the interface between weld and titanium alloy with a load of 100 g and 10 s dwelling time.

2 Results and discussion

2.1 Weld appearance

Fig. 2 displays the typical appearance of resultant Al5052/Ti6Al4V joint. It is evident from the figure that the joint surface is continuously smooth, and Ti6Al4V has been well wetted by molten AlSi12 filler metal and molten aluminum substrate giving a consistent sound lap joint. No macroscopic cracks or voids were seen on the surface of the joint and at the interface between welded seam and titanium alloy, indicating good combination of Al5052 with Ti6Al4V

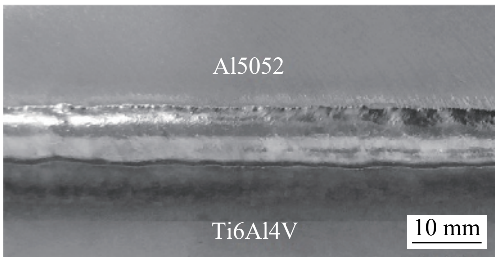

Fig. 2 Typical appearance of Al5052/Ti6Al4V welded-brazed joints

2.2 Macrostructure

The macroscopic cross-sectional view of Al5052/Ti6Al4V joint is exhibited in Fig. 3a. Under the GTAW heat source, Al alloy base metal melted and mixed with molten filler metal to form a fusion weld zone and thereafter completely spread on the Ti6Al4V surface to form a robust joint as shown in area B on the Al5052 plate in Fig. 3a. At solid-liquid interface, the interaction of Ti6Al4V with liquid mixed metal resulted in a brazed zone which is marked by area C. Thus, the joint produced by GTAW demonstrated dual features of fusion welding and brazing. A transition area combining Al5052 plate with welded seam was observed at the fusion zone, which is designated by area A.

2.3 Microstructure

Optical microstructural analysis of Al5052/Ti6Al4V welded-brazed joints is exhibited in Fig. 3b-d. A transition

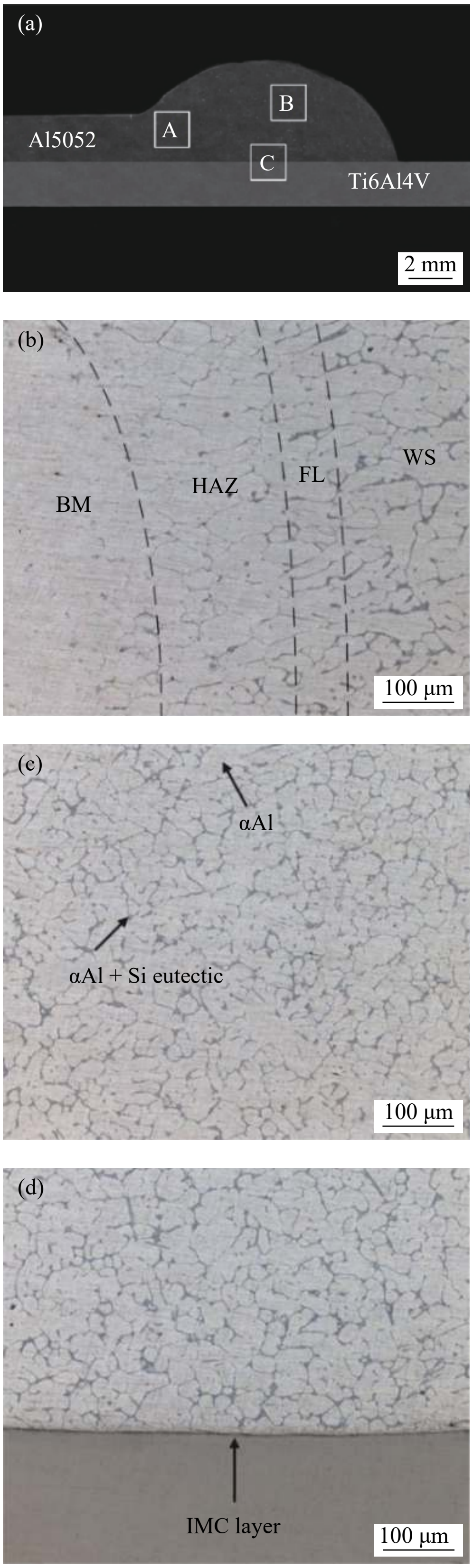

Fig. 3 Macrostructure and optical microstructures of Al5052/Ti6Al4V joint (a) Cross-sectional view and (b-d) OM images at transition region, welded seam and the interface, respectively

region marked by area A in Fig. 3a is illustrated in Fig. 3b. Four discrete regions were observed specifically which are weld seam (WS), a fusion line (FL) which is virtually vertical to the welded seam, a heat-affected zone (HAZ) area and base metal (BM). The grains were coarsened in the heat-affected zone. The HAZ microstructure featured columnar grains which were linked with fine grains of BM and coarse grains of WS. The coarsening of HAZ grains was caused by non-uniformity of the thermal cycle. Additionally, the growth trend of coarse columnar grains was nearly perpendicular to the fusion line. This specific orientation has been impelled by the large cooling rate and conductive thermal flow direction during the cooling process. Fig. 3c illustrates the microstructure of fusion welded zone (WS) as enlarged in area B of Fig. 3a and this zone contained recrystallized crystals in the process of GTAW. Chemical evaluation of the weld zone was analyzed by EDS and its results indicated that this zone is composed of α-Al grains and a eutectic phase named α-Al+Si.

Fig. 3d represents the OM image of the Al5052/Ti6Al4V brazed zone in lap joint formation which is magnified via area C in Fig. 3a. With relatively low working temperature than Ti melting point, Ti workpieces were remained unmolten or slightly melted during the GTAW process, and consequently chemically reacted with liquified filler and Al5052 to establish the brazing interface of Al5052/Ti6Al4V. Brazing occurred at the Al5052/Ti6Al4V interfacial area with the development of IMCs layer.

2.4 Microstructure of interfacial reaction zone

Fig. 4 exhibits the backscattered electron representation of IMCs layers formation at the interfacial area of Al5052/Ti6Al4V under different welding currents of 60 A to 90 A. The location where the interfacial zone was observed is specified in Fig. 1a. The welding heat input has a significant impact during GTAW process and performs an important role in the microscopic morphology of IMCs[14].

A thin serrated reaction layer can be observed at the Al5052/Ti6Al4V brazed interface which had an average thickness of approximately 1 μm at 60 A welding current as indicated in Fig. 4a. This continuous reaction layer varied directly with the heat input and grew under high heat input from interface inward to weld metal with an average thickness of 1.5 μm as displayed in Fig. 4b. Moreover, since both the temperature and diffusion interval of the reaction at interfacial area increased with a rise in welding current, this brittle IMCs layer continuously widened from 2 μm to 3.5 μm as shown in Fig. 4c and Fig. 4d, respectively. The developing path of the interfacial layer was almost vertical to the boundary of the liquid/solid interface, caused by the preferential thermal conductive course and high cooling rates[15]. The thicker IMCs reduced the quality of the joint. In order to determine the phase composition of IMCs layer, EDS investigation was conducted on the marked points 1–5 in Fig. 4 and the results are recorded in Table 3. The results obtained by EDS demonstrate that the interfacial layer is composed

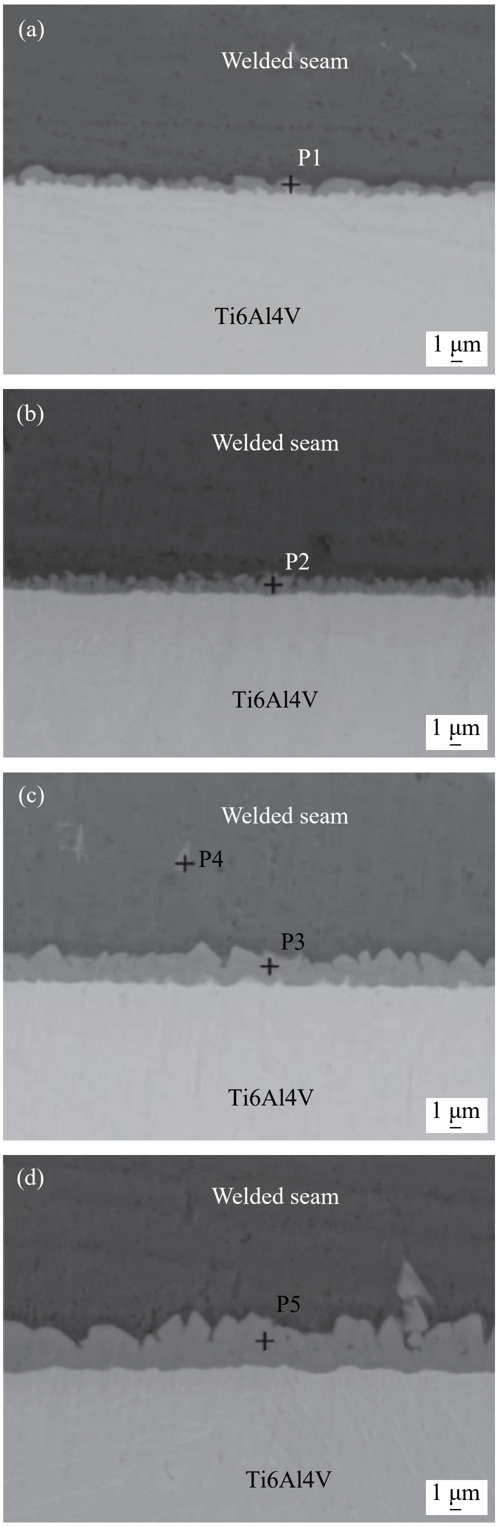

Fig. 4 Interfacial microstructures with welding currents of (a) 60 A (b) 70 A (c) 80 A and (d) 90 A

of $TiAl_3$ which is a binary intermetallic compound with up to 10% of dissolved silicon. As stated in the previous first-principles study[16], the silicon atoms have an obvious dominance to replace aluminum atoms by substitution owing to effect of energy stabilization. After formation of $TiAl_3$ IMCs layer, few Si atoms due to lower chemical potential in $TiAl_3$ diffused in the IMCs layer and afterwards ordered lattice substitution of Al by Si, $TiAl_3$ phase become $Ti(Al, Si)_3$.

Table 3 Compositional analysis at the locations marked in Fig. 4

Location	Elements (at. %)			Possible phases
	Al	Ti	Si	
P1	65.83	23.39	10.16	$Ti(Al, Si)_3$
P2	65.77	23.79	9.18	$Ti(Al, Si)_3$
P3	67.08	24.10	8.17	$Ti(Al, Si)_3$
P4	65.50	25.35	8.40	$Ti(Al, Si)_3$
P5	67.46	22.40	9.27	$Ti(Al, Si)_3$

2.5 Distribution of alloying elements

Fig. 5 shows the secondary electron images and distribution of major alloying elements Al, Si and Ti, respectively, across and along the joint interface. Depletion of Al and enrichment of silicon in the weld zone is because of the Al-Si eutectic phase formation at the grain boundary and it's verified via elemental distribution mapping as displayed in Fig. 5b and Fig. 5c, respectively. It can be seen in Fig. 5d that with welding current of 60 A, Ti atoms diffused into the interfacial layer due to heat conductivity of welding arc and after formation of IMCs some of Ti appeared in the weld zone as $Ti(Al, Si)_3$ phase marked by elliptical zones. With low welding current relatively, the optimum temperature that brazed area of Al5052/Ti6Al4V experienced was low and, however, cooling rate of workpiece was high. Consequently, due to short reaction time, a fine serrated reaction layer formed at the Al5052/Ti6Al4V interface as shown in Fig. 5a. This mapping also showed that the interfacial layer contained Al, Si and Ti. Si atoms concentrated at the interface between titanium and weld due to reduction in chemical potential of silicon which was induced by the Ti dissolution. With further increase in welding current up to 70 A, dissolving rate of Ti6Al4V was high due to higher heat input and increased diffusion of Ti in the liquified mixed metal. As a result, the brittle IMCs accumulated and grew deeply into the weld zone as indicated by elliptical zone in Fig. 5h. These brittle IMCs influenced the mechanical properties of the joint.

2.6 Joint strength and fracture analysis

Fig. 6 represents the tensile shear strength of Al5052/Ti6Al4V welded joints. Owing to the asymmetrical configuration of the tensile test specimens, the joints experienced both shear and tensile forces during the tensile test. Therefore, the strength of the joint was given in N/mm, because it was complicated to separate both stresses[17]. The welding current performed an influential role on mechanical strength of the joint. Welding current of 50 A failed to

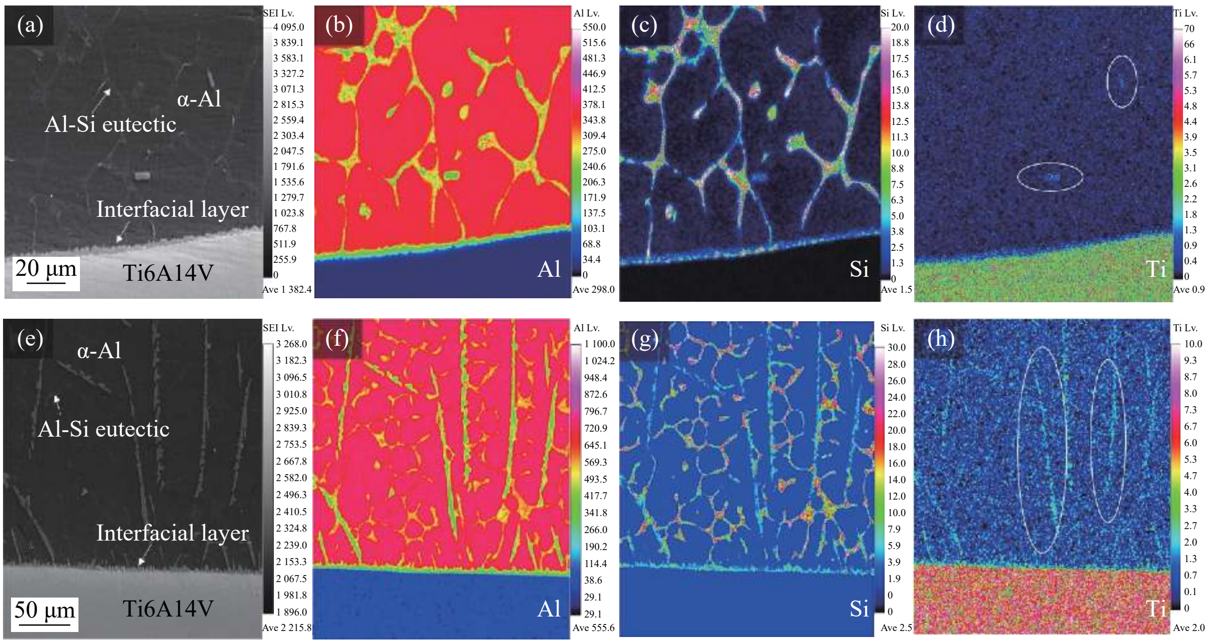

Fig. 5 SEI images and elemental distribution of aluminum, silicon and titanium across the Al5052 / Ti6Al4V interface: (a-d) and (e-h) at 60 A and 70 A welding current, respectively

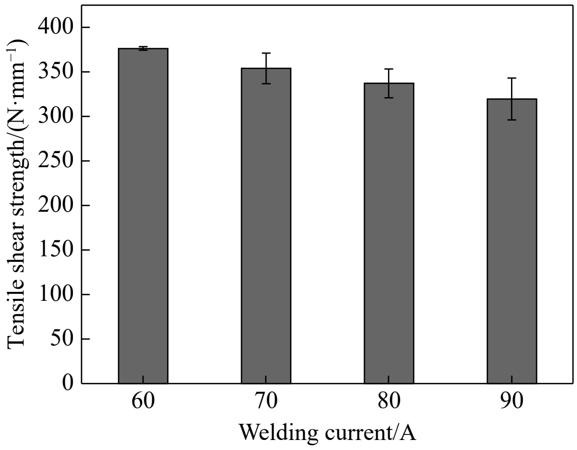

Fig. 6 Tensile shear strength of the joints with varied welding currents

provide adequate heat and sufficient spread of molten filler on Ti6Al4V substrate. So, during the machining of the tensile specimen, sample broke. However, the excellent bonding strength was achieved with optimized 60 A welding current and the optimal joint performance appeared with an average value of 376 N/mm along with the formation of thin IMCs layer. Nonetheless, at 70 A welding current, the joint shear strength decreased comparatively due to thicker interfacial reaction layer and the melt of Ti6Al4V substrate. The brittle continuous IMCs further grew thicker at the interface and deeper in the weld zone due to high heat input with welding current from 80 A to 90 A which resulted in the occurrence of Al alloy explosion and further reduction of joint shear strength.

Fig.7, Fig.8 and Fig.9 illustrate the fracture phenomena and surface analysis of Al5052/Ti6Al4V lap joint welded with varied welding heat input. The representative images showed that the rupture behavior of the joints intimately correlative to the welding current. With optimized welding current of 60 A, the resultant joint endured plastic fracture under the tensile-shear forces and fractured from the Al base metal as shown in Fig. 7a. Fig 7b demonstrates that the ductile fracture surface morphology of the robust joint was distinguished by equiaxed dimple patterns. At the welding current of 70 A, the joint fractured near the Al5052/Ti6Al4V interface as indicated in Fig. 8a. During the high heat input, the IMC layer grew from the interface towards

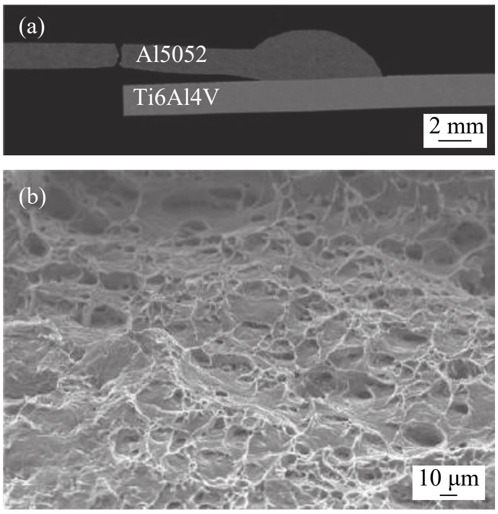

Fig. 7 Fraction phenomena of Al5052/Ti6Al4V joint at 60 A welding current (a) Fracture location (b) Fracture surface

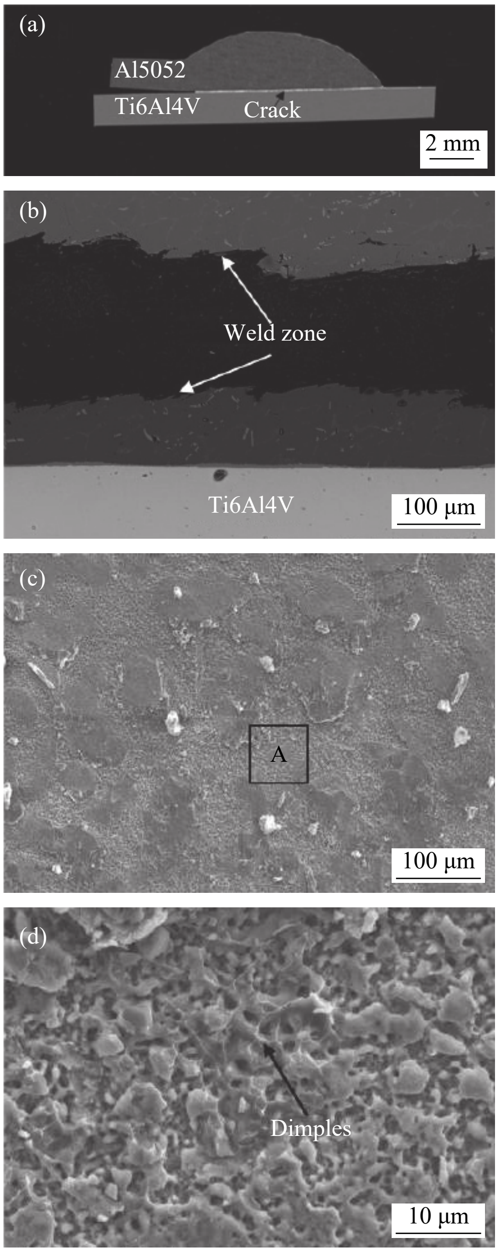

Fig. 8 Fracture location (a) Fracture path (b) Fracture surfaces at titanium alloy side of the joint (c) (d) at 70 A welding current

the weld zone and hence this weld zone close to interfacial layer was the weakest part of the joint due to increased concentration of $Ti(Al, Si)_3$ phase as depicted in Fig. 8b. Fig. 8c presents the fracture surface of the specimen which contained scraggly and smooth regions. The scraggly areas are characterized by lamellar tearing pattern, indicating the brittle fracture along with the plastic deformation at some areas as marked by area A and magnified in Fig. 8d. Dimples are observed on the fractured surface. The surface morphology indicates the mixed fracture of brittle and plastic deformation occurred during the tensile test. Moreover, when the welding current raised from 80 A to 90 A, Ti alloy molten due to high heat input causing the IMCs layer grew thicker due to which crack initiated and propagated through interfacial layer. Fig. 9b represents the surface morphology of Al5052/Ti6Al4V fractured joint at 90 A. The fractured surface reveals a quasi-cleavage fracture with lamellar tearing pattern and brittleness of the joint caused by fractured path via interfacial layer as depicted in Fig. 9a.

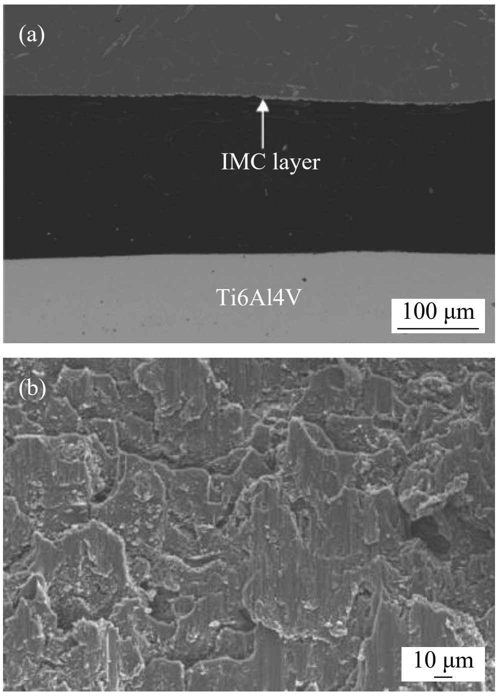

Fig. 9 Fracture path of Al5052/Ti6Al4V joint (a) and fracture surface at titanium alloy side of the joint (b), respectively, at 90 A welding heat input

2.7 Microhardness

The microhardness test results of the Al5052/Ti6Al4V joint at 60 A in transition area and across the interface are exhibited in Fig.10. Fig. 10a clearly shows that the hardness value increased in HAZ. The average hardness of HAZ with a value of 90 HV was comparatively higher than that

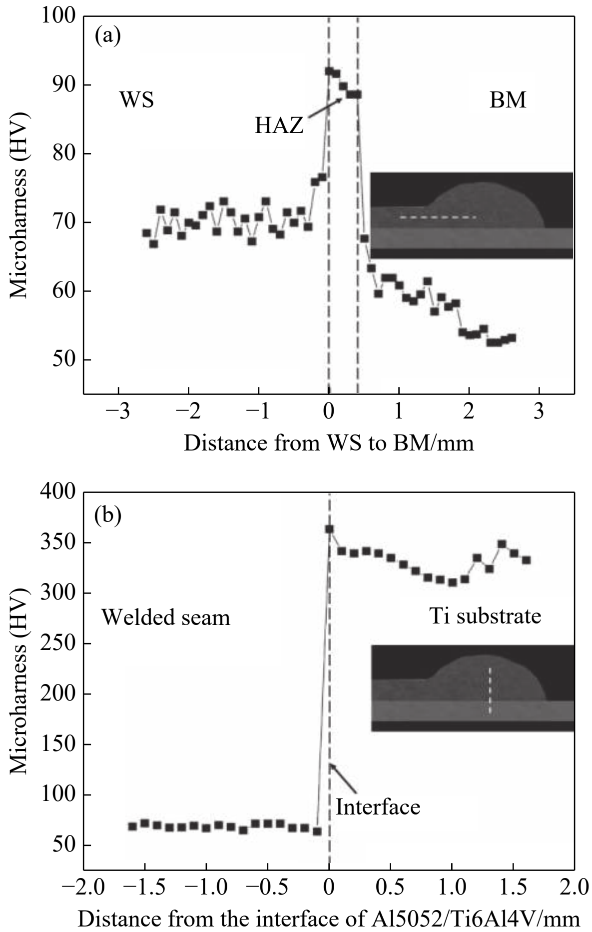

Fig. 10 Hardness variations in Al5052/Ti6Al4V joint at 60 A welding current (a) Fusion zone (b) Across the interface

in Al base metal (BM). The grains slightly elongated in the HAZ, but this region is shortened as a result of lower welding heat input which is in turn advantageous for mechanical strength of the welded joints. Thus, the HAZ was not the weakest part of the joint and sound joint has been produced. Fig. 10b presents the hardness distribution across the interface of Al5052/Ti6Al4V joint. It shows that the hardness of Ti6Al4V with average value of 310 HV is considerably greater than that of the welded seam (70 HV). However, the hardness (363 HV) at the interface of Al5052/Ti6Al4V was higher than both of welded seam (WS) and Ti6Al4V owing to the development of $Ti(Al, Si)_3$ phase. The $TiAl_3$ phase is rigid[18]. Though, the microhardness of IMCs layer is ascribed to the existence of distributive phase of Al and a certain level replacement of Al atoms by Si atoms in the brittle $TiAl_3$.[19]

3 Conclusion

(1) At the Al5052/Ti6Al4V interface, an uneven serrated reaction layer consists of brittle phase $Ti(Al, Si)_3$ with

about 10 at. % silicon solubility was formed due to the interaction of titanium with liquefied filler.

(2) The thickness of interfacial reaction layer increased with a rise in welding heat input, and the mechanism of interfacial layer development was directed by dissolution of titanium atoms and their diffusion in the melted AlSi12 filler wire.

(3) At elevated welding currents, the thickness of IMCs layer increased, which weakened the mechanical strength of the joint.

(4) The maximum tensile shear strength 376 N/mm of robust joint was obtained at welding current of 60 A, and the joint fractured from the aluminum alloy base metal. The fracture morphology of optimized joint is featured by equiaxed dimple patterns.

(5) The microhardness measurement displayed that the hardness at the interface of Al5052/Ti6Al4V was higher than that in the weld seam and Ti6Al4V substrate owing to the formation of brittle IMCs.

References

[1] Chen B, Xiong H, Sun B, et al. Microstructure evolution and tensile properties of Ti3Al/Ni-based superalloy welded joint. Journal of Materials Science and Technology, 2014, 30(7):715 − 721.

[2] Atieh A M, Khan T I. Transient liquid phase (TLP) brazing of Mg–AZ31 and Ti–6Al–4V using Ni and Cu sandwich foils. Science and Technology of Welding and Joining, 2014, 19(4):333 − 342.

[3] Ma Z, Wang C, Yu H, et al. The microstructure and mechanical properties of fluxless gas tungsten arc welding-brazing joints made between titanium and aluminum alloys. Materials & Design, 2013, 45:72 − 79.

[4] Möller F, Grden M, Thomy C, et al. Combined laser beam welding and brazing process for aluminium titanium hybrid structures. Physics Procedia, 2011, 12:215 − 223.

[5] Chen S H, Li L Q, Chen Y B, et al. Joining mechanism of Ti/Al dissimilar alloys during laser welding-brazing process. Journal of Alloys and Compounds, 2011, 509(3):891 − 898.

[6] Wan L, Lü S, Huang Y, et al. Effect of hot dip aluminising on interfacial microstructure and mechanical properties of Ti/Al joint by TIG arc welding brazing. Science and Technology of Welding and Joining, 2015, 20(2):164 − 171.

[7] Takemoto T, Okamoto I. Intermetallic compounds formed during brazing of titanium with aluminium filler metals. Journal of Materials Science, 1988, 23(4):1301 − 1308.

[8] Fronczek D M, Wojewoda-Budka J, Chulist R. Structural properties of Ti/Al clads manufactured by explosive welding and annealing. Materials & Design, 2016, 91:80 − 89.

[9] Jiangwei R, Yajiang L, Tao F. Microstructure characteristics in the interface zone of Ti/Al diffusion bonding. Materials Letters, 2002, 56(5):647 − 652.

[10] Kimura M, Nakamura S, Kusaka M, et al. Mechanical properties of friction welded joint between Ti–6Al–4V alloy and Al–Mg alloy (AA5052). Science and Technology of Welding and Joining, 2005, 10(6):666 − 672.

[11] Wang H, Yuan X, Li T. TIG welding-brazing of Ti6Al4V and Al5052 in overlap configuration with assistance of zinc foil. Journal of Materials Processing Technology, 2018, 251:26 − 36.

[12] Xu C, Sheng G, Wang H, et al. Effect of high energy shot peening on the microstructure and mechanical properties of Mg/Ti Joints. Journal of Alloys and Compounds, 2017, 695:1383 − 1391.

[13] Xu C, Sheng G M, Deng Y Q, et al. Microstructure and mechanical properties of tungsten inert gas welded–brazed Mg/Ti lap joints. Science and Technology of Welding and Joining, 2014, 19(5):443 − 450.

[14] Chen Y B, Chen S H, Li L Q. Effects of heat input on microstructure and mechanical property of Al/Ti joints by rectangular spot laser welding-brazing method. The International Journal of Advanced Manufacturing Technology, 2009, 44(3 − 4):265 − 272.

[15] Lü S X, Jing X J, Huang, Y X, et al. Investigation on TIG arc welding–brazing of Ti/Al dissimilar alloys with Al based fillers. Science and Technology of Welding and Joining, 2012, 17(7):519 − 524.

[16] Zhu G, Dai Y, Shu D, et al. Substitution behavior of Si in Al_3Ti (D0 22): A first-principles study. Journal of Physics: Condensed Matter, 2009, 21(41):415503.

[17] Li L, Tan C, Chen Y, et al. Comparative study on microstructure and mechanical properties of laser welded–brazed Mg/Mild steel and Mg/stainless steel joints. Materials & Design, 2013, 43:59 − 65.

[18] Guo B, Zhou J, Zhang S, et al. Tribological properties of titanium aluminides coatings produced on pure Ti by laser surface alloying. Surface and Coatings Technology, 2008, 202(17):4121 − 4129.

[19] Akhtar A, Dong H G, Xia Y Q, et al. Lap joining Al5052 to Ti6Al4V by GTAW with AlSi5 filler wire. China Welding, 2019, 28(2):15 − 23.